Handbook of Advances in Life Sciences

Handbook of Advances in Life Sciences

Edited by

Jill Shukla

Cambridge Scholars Publishing

Handbook of Advances in Life Sciences

Edited by Jill Shukla

This book first published 2023

Cambridge Scholars Publishing

Lady Stephenson Library, Newcastle upon Tyne, NE6 2PA, UK

British Library Cataloguing in Publication Data
A catalogue record for this book is available from the British Library

ISBN (10): 1-5275-9451-3
ISBN (13): 978-1-5275-9451-7

TABLE OF CONTENTS

FOREWORD

The Handbook of Advances in Life Sciences is a performance-based text intended for use by researchers of various fields like Pharmacy, Genetics, Biotechnology, Environmental Toxicology, Conservation Biology, Entomology, Microbiology and Allied Sciences, as well as anyone interested in Life Science. Research in life sciences is increasingly becoming interdisciplinary in developing countries. Interdisciplinary life sciences integrate multiple disciplines in the search for solutions to multifaceted problems under the general umbrella complex of biological systems. Biology seems to be the centerpiece of life science, while molecular biology and biotechnology advancements have led to the burgeoning of specialization and new interdisciplinary research. The book is lavishly illustrated with flow charts, diagrams, and tables for easy learning. Original research by the authors is also included in the book. Through the book, we have attempted to provide a considerable amount of information from the vast and ever-growing field of life science.

CHAPTER 1

THE SKELETON FOR TOPOLOGICAL AND METRIC SHAPE MEASUREMENT

JOHN C. RUSS[1] AND F. BRENT NEAL[2]

[1]Professor Emeritus, Materials Science Dept., North Carolina State Univ., Raleigh, NC, Email: jruss@ncsu.edu

[2]Technical Manager, North America Wood Coatings, AkzoNobel N.V., High Point, NC, Email: brentn@gmail.com

Abstract

The shape of objects is important for identification and correlation with history or properties, but difficult to measure effectively. Landmark methods and dimensionless ratios capture only overall form, and boundary representations such as Fourier or wavelet coefficients are too numerous for ready human understanding. The skeleton provides a complete description and offers simple topological and metric measures that are especially useful for biological specimens. Examples are presented.

Keywords: Skeleton, medial axis, topology, measurement, shape

Introduction

Shape is an important attribute of objects, but not easily measured; a wide variety of methods have been proposed and utilized [Loncaric, 1998; da Fontoura Costa & Cesar, 2009; Neal & Russ, 2012]. Deriving numerical values to measure shape for identification, characterization, or correlation to history or behavior, is sometimes performed by selecting, either by eye or automatically, landmarks that describe the basic form, or by representing the boundary of a 2D or 3D object or structure, for example using Fourier or wavelet techniques. The advantage of these latter methods is that the

characterization is complete (the shape boundary can be exactly reconstructed), but statistical methods select just those few of the many numbers which are found to be sufficient for a particular purpose. There is a different approach to shape measurement, also complete and able to reconstruct the original shape, which lends itself to extracting a few readily understandable topological and metric values for analysis. This skeleton or medial axis is the set of connected midlines that represent the topology, which human observers generally associate with shape, especially for objects that are not compact but have extensions from a main body, or are extended networks. The skeletons also contain metric information: the lengths and orientations of the branches, their curvature, and the spacings of the nodes and end points. Distance values to the boundary along the skeleton measure the local width dimensions of the original shape. Constructing the skeleton or medial axis is efficient, and the measurement operations are straightforward. Their use for analyzing structures can provide additional insights into the interpretation of shapes. This is especially true for, but is not limited to, branching structures, and for biological subjects that share important aspects of shape but are not exactly identical or may appear in different poses. Both macroscopic and microscopic examples are illustrated.

Landmarks and Procrustes matching

The Procrustes method for measuring shape differences (*e.g.*, between two or more possibly different specimens or groups of specimens) has often been used in biological applications and is generally described [Klingenberg, 2015] as shown in Figure 1. The landmark points shown in the figure are features (vein junctions in insect wings) considered to be significant. Often, landmark points are placed along the perimeter, or a portion of the border. For instance, in comparing profiles of skulls, many points are used to define the top but few are placed across the bottom. Human judgment selects landmarks that are considered to be visually or structurally important. The shape to be compared is first scaled to be the same size as the target (which may be another similar image, or a presumed "mean" shape), then shifted to the same position and rotated to align with it. But there are many different options for each of these steps, which influence the quality and meaning of the result.

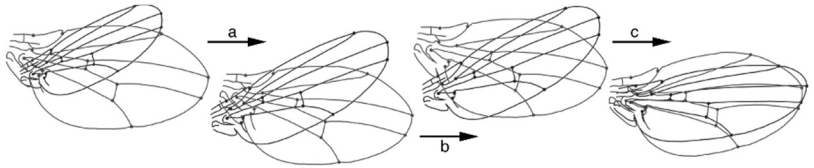

Figure 1. Sequence of steps in Procrustes superimposition: a) scaling, b) shifting, c) rotating, followed by measuring the distances between corresponding landmarks.

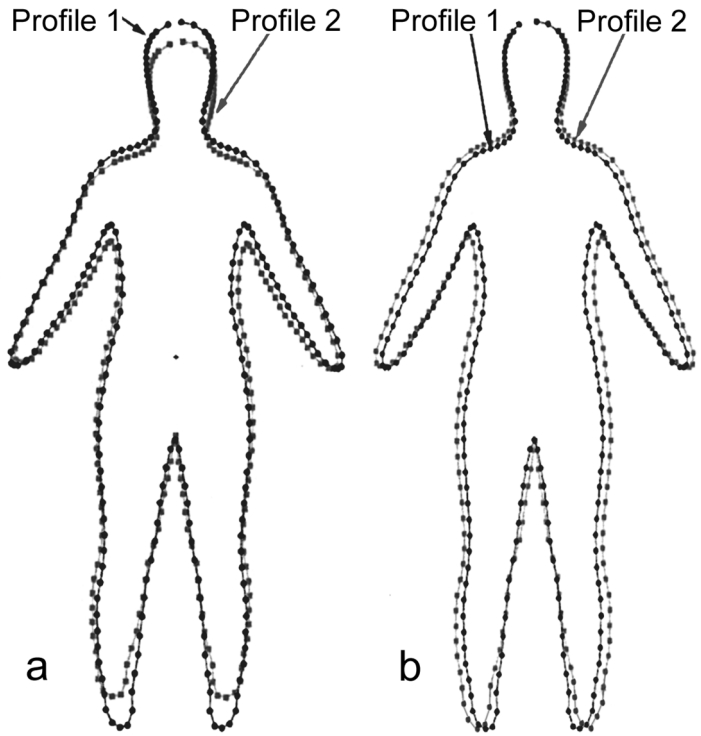

Figure 2. Comparing frontal outlines with different scaling methods: a) area matching; (b) height matching.

First, size matching may be done based on the total area of the object, or the length of an ellipse fit to the landmark points, or the distance between two landmark points, usually at extreme positions. The latter case is especially used when two points are chosen to mark the ends of an axis considered important. This is often a vertical or horizontal axis, for example the tips of the ears when aligning face images, or the top of the head and bottom of the

feet when aligning whole-body views. Figure 2 compares the results of scaling based on area vs. matching the length of the vertical distance [Lestrel *et al*., 2017].

Translation typically aligns the centroids, but this may be either based on the area, or the marked landmark points, or a subset of those (*e.g*., the middle of a marked axis). If the two-point axis method is used, this axis is often also used for the alignment step, but for more general shapes the alignment may be based on the axis of the ellipse used for size matching. Rotational alignment may also use other selected landmarks. If the landmark points lie along the periphery, and especially if they are concentrated in just a portion of the full outline, they may strongly bias the alignment.

A final refinement of the size scaling, position adjustment, and/or rotational alignment may be added to minimize the combined distances between the corresponding landmark points. Then the distances, and sometimes the directions, are used as a measure of shape differences. The measure of difference may be further reduced to the square root of the sum of squares of the straight line distances between the pairs of corresponding landmarks. If some of the points are considered more important than others they may be given greater weights, and in some instances the distances in a specific direction (*e.g*., perpendicular to the selected axis used for scaling and alignment) may be used.

With so many variations, and considering the human element in choosing procedures and landmark placement, and the fact that these points are often non-uniformly distributed within or around the shapes, it is not surprising that there is no generally applicable metric that can be used to relate the final result to a shape difference. But for comparing specific populations, or matching samples to an accepted standard, the final measurement parameters may be used in statistical tests.

Fourier analysis

Measurement of shape often relies on the boundary. Indeed, Lestrel [1997] has explicitly stated that: “Shape is a boundary phenomenon. It refers to the boundary outline of a form in 2D or 3D. Its focus is on curvature.” Bookstein [1978] went even farther, defining shape as: “... an outline with landmarks from which all information about position, scale and orientation has been drained.” This may seem to be an obvious description, since it is the boundary or surface of an object that we see, and extracting the boundary from the image of an object can usually be accomplished by image

processing operations, yielding a linked line of pixels (in 2D) or a contiguous set of voxels (in 3D) whose size and spacing define the image resolution. In order to represent these arrays mathematically, tools such as Fourier or wavelet analysis in 2D and spherical harmonic or wavelet analysis in 3D are common approaches.

The original approach [Ehrlich & Weinberg, 1970] to Fourier analysis of shapes "unrolls" the outline of an object by plotting radius as a function of angle from the centroid (Figure 3). This profile is then expressed as the usual Fourier series of sine and cosine or amplitude and phase, and in many instances the phase is ignored and the first few (*e.g.*, 20-50) power terms (square of the amplitude) are used as a measure of shape. This approach requires the function to be single-valued and continuous, and so cannot handle re-entrant or disconnected shapes that cause multiple intersections of the profile with the radial line at some angles.

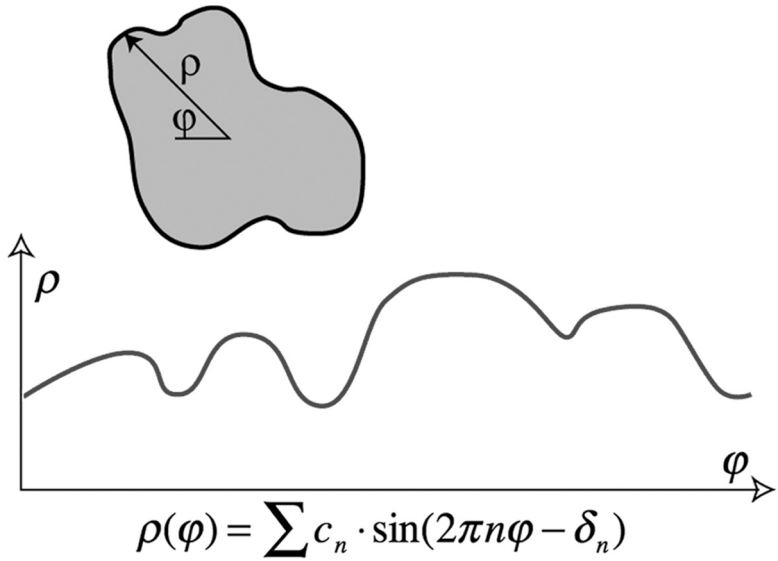

Figure 3. "Unrolling" a shape by plotting radius from the centroid as a function of angle.

One solution to this problem is to separately plot the x-coordinates and y-coordinates of points along the outline, as shown in Figure 4, and perform Fourier analysis on each of those functions [Iwata & Ukai, 2002]. This produces four columns of the coefficients (*a, b, c, d*) as a function of

frequency for the first 20-50 terms. Normalizing the coefficients based on the size of the first order amplitude removes size information and makes the data purely shape dependent. The distribution of power vs. frequency may be used to analyze characteristics at different dimensional scales, but in most cases the numbers are treated *in toto* as a description of shape. The data from the measurement of a population of objects, or objects that may belong to more than one population, are fed to a statistical analysis procedure such as principal components analysis. If the first few principal component values for a series of measured objects has a high statistical significance and shows that presumed different populations are well separated, or conversely if they cannot be distinguished, that may be taken as an indication or even proof that the populations are (or are not) distinct.

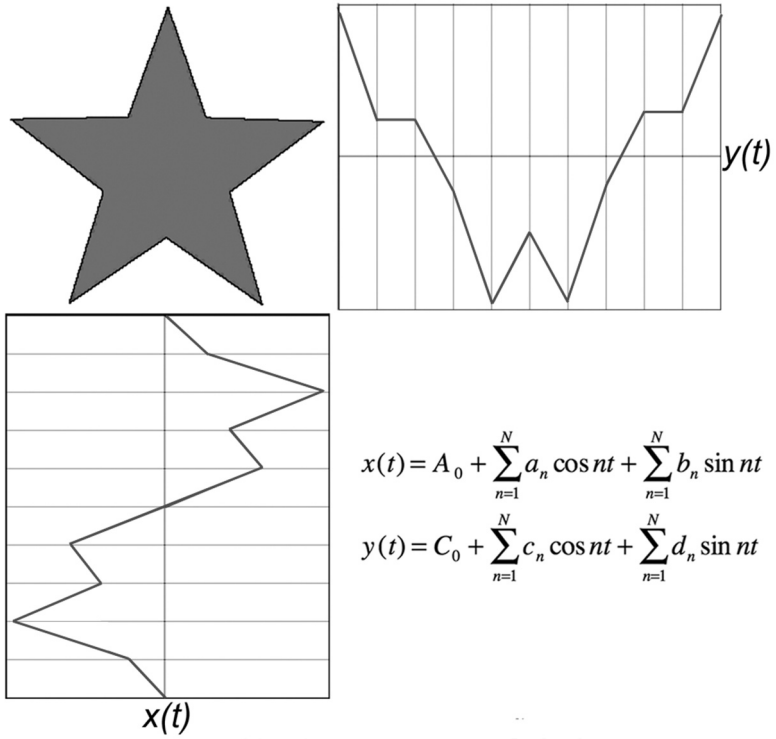

Figure 4. The elliptical Fourier method, projecting the x- and y-profiles of a shape and performing separate Fourier analysis on each to produce 4 sets of values.

The equations of the linear combinations of the various *a, b, c, d* amplitudes that constitute the principal components are rarely shown, and almost never is an interpretation of their meaning proposed. In some instances, the averages of the values for a population are used to draw a "mean" shape, and the ±2 standard deviation values of those terms used to draw outlines to illustrate the variation of shapes within the population (if the frequency terms for the different projections do not vary independently this is an incorrect interpretation). The resort to using the drawn "representative" outlines places the interpretation back on the visual judgment of the human observer. Visually comparing the mean shape outlines for two populations that PCA calculation has indicated may be distinguished invites comments such as "the important difference between the two species can be seen at the tips of the limbs."

A simpler method unrolls the outline based on the change in the local slope or direction as a function of distance along the boundary [Zahn & Roskies, 1972]. As shown in the Figure 5, this method assigns an integer (1–8) to the possible directions linking each pixel along the edge to the next one. The chain code values cannot be used directly for Fourier analysis because of the discontinuity produced by a step from 8 to 1, but converting to differential chain code solves this difficulty: for each step in the chain, a value of 0 indicates that there is no change in direction from the preceding link, while a value of plus or minus one indicates a change inward or outward of 45 degrees (±2 indicates a 90 degree step, ±3 a rare 135 degree step). This series of values has no discontinuities, and also makes the shape representation rotationally independent. A minor objection to using this series for Fourier analysis is that the points are not uniformly spaced (the distance between pixels in the 45 degree directions is 41% greater than in the 90 degree directions); this can be adjusted by padding. If the integer differential chain code is too discrete and noisy, applying a weighted smooth to the values is quick and effective.

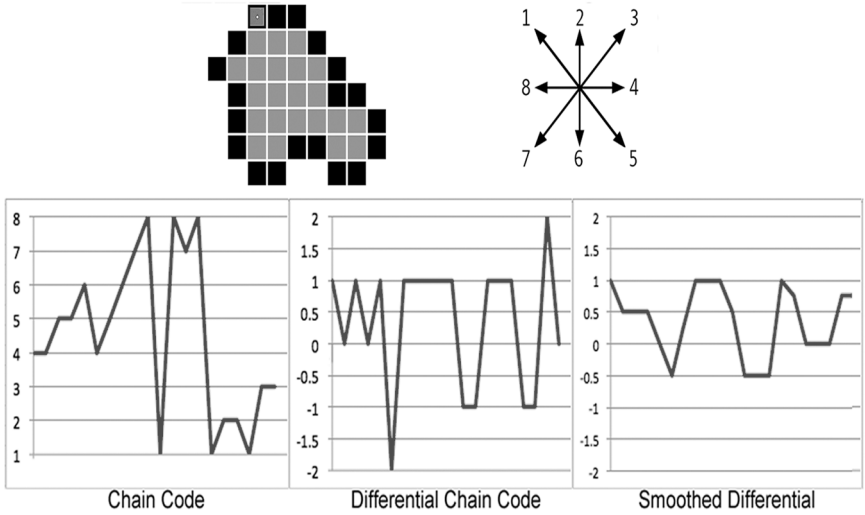

Figure 5. A tiny shape with its chain code, differential chain code, and smoothed differential chain code.

The resulting Fourier analysis coefficients, usually shown as amplitude and phase, can be interpreted to show the importance of specific frequencies to the irregularities in the profile of the object, and used to reconstruct the profile. They can also, of course, be used for the same statistical tests, and mean profiles drawn for visual comparison. This approach cannot be applied to 3-D shapes, but 3-D harmonic analysis with Legendre polynomials or spherical harmonics [Brechbühler *et al*., 1995] produces analogous results.

Wavelet analysis

Wavelet analysis [Brechbühler *et al*., 1995] is another common approach to representing boundaries, applicable to both 2-D and 3-D objects. It produces a spectrum showing both the relative importance of various spacings or periodicities (akin to the frequencies in a Fourier series) and also their localization on the boundary of the shape as illustrated in Figure 6. This localization is often very important, since many shapes have different characteristics along different regions of their periphery. Analysis of a wavelet spectrum may extract significant terms based on either spacing or location, or both.

With these methods, and other techniques that represent a contour as a collection of defined forms [Drolon *et al*., 2000], the number of values sufficient to fully reconstruct the object outline may approach the number of pixels or voxels on the original boundary or surface. Teasing out the significant (few) numbers that are useful for an identification or correlation task typically requires a multivariate statistical approach. It is not often that the resulting parameters derived from the raw data are readily understandable or apparent to a human observer, even if the visual appearance of the objects in question can be more-or-less satisfactorily used for identification, comparison or correlation. In short, the success and utility of the boundary analysis does not satisfy a desire to understand what the numbers "mean," and there is generally no consistency in which few numbers or combinations of numbers are selected as statistically useful in different instances.

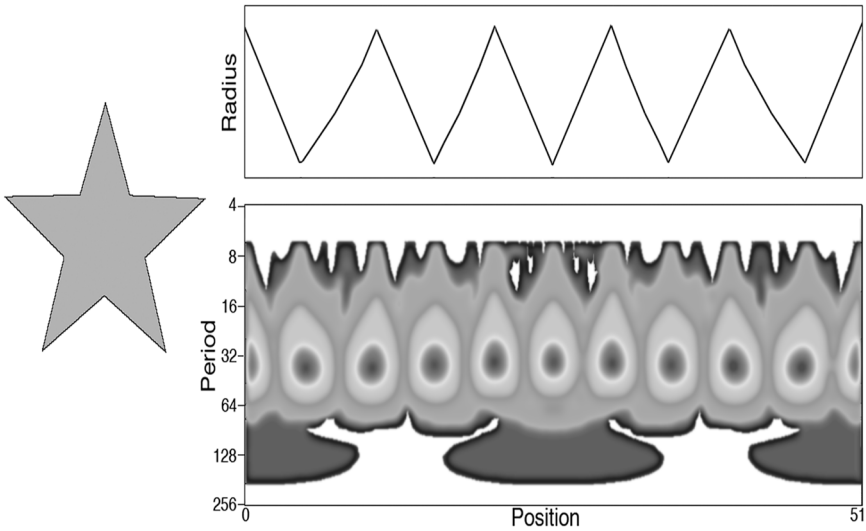

Figure 6. Wavelet spectrum for an unrolled star shape, indicating the spacings and location of boundary irregularities.

Dimensionless ratios

At the other extreme, in the "early days" of image processing when computing power was limited, shape description generally used dimensionless ratios of size measures, such as length divided by breadth (called aspect ratio, but dependent on just how the length and breadth are defined). One of the most widely used "shape factors," still reported by

many image analysis programs, is 4π•Area / Perimeter^2, which goes by various names such as formfactor, circularity, roundness, etc. A few additional common shape factors are listed in Table 1. Analogous ratios can be devised for 3D objects. These ratios cancel out any dimensional units and so are independent of object size, except as it affects the measurement precision. For many objects the measured value of perimeter (or surface area) typically increases as resolution increases and reveals more boundary irregularities, and this affects those ratios that use the perimeter. (Of course, this same effect is present for all shape characterization methods that depend on the boundary.) It is also necessary to decide whether the perimeter and area values include the boundaries and areas of any holes in the object.

Table 1. Some Dimensionless Shape Descriptors

$$Formfactor = \frac{4\pi \cdot Area}{Perimeter^2}$$

$$Aspect\ Ratio = \frac{Length}{Breadth}$$

$$Elongation = \frac{4 \cdot Area}{\pi \cdot Length^2}$$

$$Solidity = \frac{Area}{Convex\ Hull\ Area}$$

$$Convexity = \frac{Perimeter}{Convex\ Hull\ Perimeter}$$

$$Radius\ Ratio = \frac{Inscribed\ Radius}{Circumscribed\ Radius}$$

The principal objection to the dimensionless ratios for shape measurement is that they are not unique and many visually different shapes can have the same value of one or several of these ratios. On the other hand, when the selection of one or a few of these ratios is found that effectively distinguishes classes of objects, as illustrated in Figure 7 [Neal & Russ, 2012], or shows a correlation with some property, they are extremely efficient as shape descriptors, and generally understandable to the human user since the size measures on which they are based are more-or-less familiar. Procrustes, Fourier or wavelet methods for shape description have increasingly replaced this approach, although in many applications these

simple ratios perform at least as well as the more computer-intensive methods.

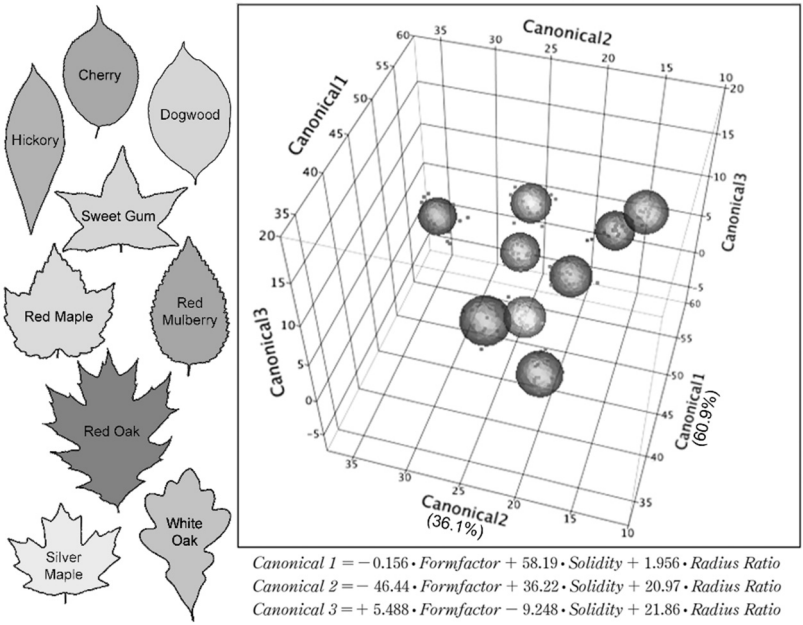

Figure 7. Example of identification of leaves based on dimensionless ratios as shape descriptors. The overall error rate is less than 2%.

The skeleton

A very different approach can also be employed to measure shape, generating a different data set and in some cases leading to a more readily understandable small number of measurement values. It is based on the skeleton (or medial axis, the terms are used interchangeably here) of the object. This is not a new concept; it is mentioned in numerous early publications [Blum, 1967; Bookstein, 1978], and has been employed in a variety of very different applications over the years. But skeletons have been underutilized for shape measurement as interest has instead been focused on boundary description. The skeleton is especially appropriate for biological subjects since individuals within a class often share basic characteristics but

are rarely exactly similar, and furthermore may appear in different poses which alter the details of the outline but not the basic skeletal information.

Human vision responds strongly to topology as a descriptor of shape [Lowet *et al*., 2018], which is captured directly by the skeleton. For digitized representations in either 2D or 3D, the skeleton is the set of points (pixels or voxels) that lie at equal distances from separated boundary points. The skeleton is a connected line of pixels or voxels, in which the removal of any one would cause the line to become disconnected. In 2D this usually consists of a pixels that are "8-connected," meaning that they touch their neighbors either along their four sides or at their four corners (Figure 8a). In 3D the voxels are ideally "26-connected" touching along any of the six faces, twelve edges or eight corners (Figure 8b), but in many practical implementations a simpler procedure produces lines that are only considered to be connected along the six voxel faces ("6-connected," Figure 8c). The medial axis is the most often used topological representation, but in 3D there is also a medial surface which retains information about twists in a structure. This is less commonly used and generally more difficult to analyze (Figure 9).

There are several algorithms to construct the medial axis [Siddiqi & Pizer, 2008; Saha *et al*., 2017], for instance by iterative removal of pixels or voxels that touch the surrounding background and whose neighbors also touch each other [Pavlidis, 1980]. The skeleton is also related mathematically to the Fourier descriptors of the boundary, and can be derived from it for many 2D shapes [Persoon & Fu, 1977]. Relationships to surface representations can also be extended to general 3D shapes [Vermeer, 1994].

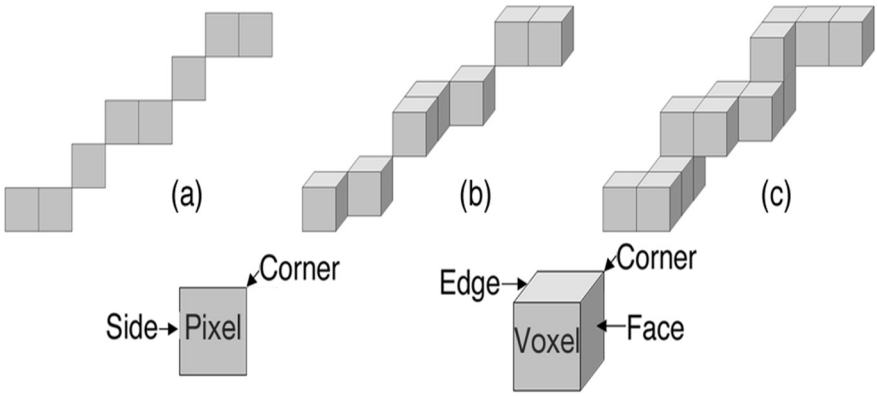

Figure 8. Connected lines of pixels and voxels: a) 8-connected in 2D; b) 26-connected in 3D; c) 6-connected in 3D.

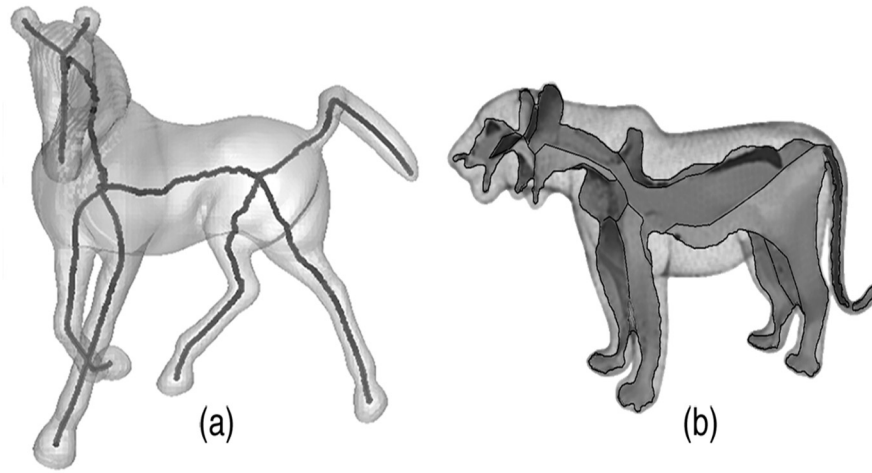

Figure 9. The medial axis (a) and the medial surface (b) of 3D objects.

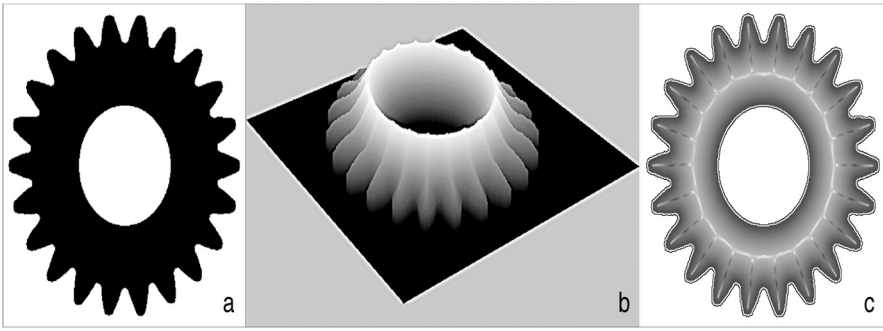

Figure 10. Constructing the EDM and medial axis: a) an example shape; b) the Euclidean distance values represented as elevation at each point within the shape; c) the ridges in the EDM values marked with colors to show the values of the medial axis.

An efficient method for deriving the skeleton, and the one that often produces the most useful result, is based on the Euclidean distance map (EDM) [Danielsson, 1980; Shih & Fu, 1995; Malandain *et al*., 1998], a processing operation that assigns to each pixel or voxel a value equal to the straight line distance to the nearest surrounding background pixel or voxel. In Figure 10, the EDM values are shown as a rendered elevation at each point; the ridge lines where the maximum downhill gradients point in two different directions constitute the medial axis. The combination of the skeleton location and the distance values along it is the medial axis transform (MAT). Marking those locations with a color representing the distance is a useful way to show the result.

Many image processing programs can generate the EDM and the MAT or skeleton, and there is an extensive literature describing algorithms and implementation, some of which produce a skeleton that is more robust to the presence of minor irregularities in the external contour [Feldman & Singh, 2006; Shen *et al*., 2016]. Neural nets have been utilized to derive skeletons of component parts in pixel images [Shen et al., 2011] but this is concerned more with segmentation than object shape measurement.

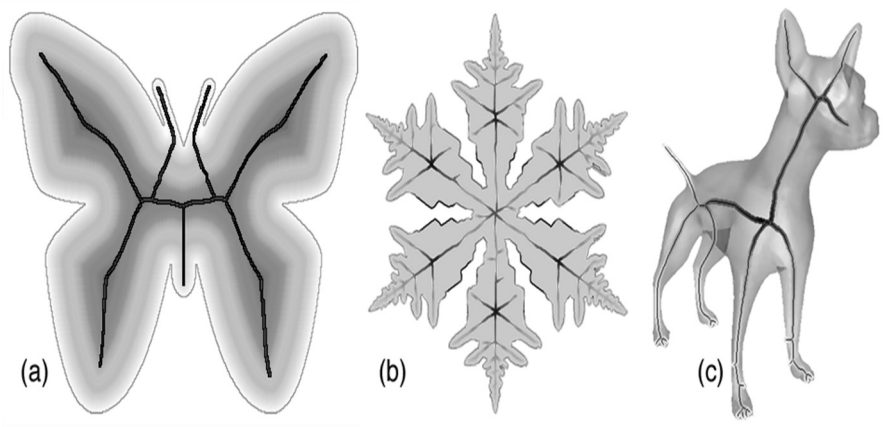

Figure 11. Representing shape with the medial axis transform: a) a simple 2D shape with the color-coded EDM and the superimposed skeleton; b) a complex 2D shape with the values of the distance map shown as color coding in the MAT and along the outline; c) the color-coded MAT values for a 3D object.

As shown in Figure 11 for several shapes, the MAT values have a ridge or axis of maximum values that define the skeleton, and record the radius of the inscribed circle (or sphere, in 3D) at each point. Superimposing the circles or spheres centered at each point on the MAT with the corresponding radius regenerates the complete shape, as indicated in Figure 12. Although the MAT is a complete record of the shape, many of the circles overlap others, so that this is not an efficient representation; in most cases, the Fourier description of the boundary is a more efficient coding [Leonard, 2007]. Graph theory offers some possibilities for analysis, for instance by constructing a matrix of node and end connections, with branch lengths and widths [Bardinet *et al*., 2000; Di Ruberto, 2004; Zhang *et al*., 2005; Macrini *et al*., 2008].

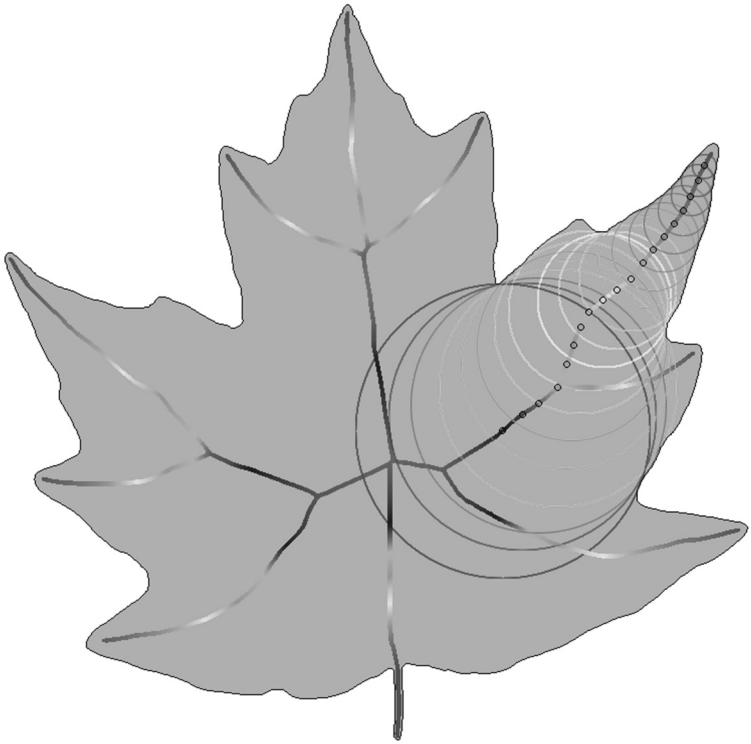

Figure 12. Shape (a silver maple leaf) with its color-coded medial axis transform and a few of the circles which superimpose to regenerate the complete shape.

A related approach organizes the data into a shock graph [Siddiqi *et al*., 1999; Leymarie, 2003; Rezanejad & Siddiqi, 2013] as shown in Figure 13; the marked locations are classified into one of four kinds of "shocks" (the terminology comes from representation of the distance map as a heat diffusion equation) related to the local boundary curvature and hence to the derivative of the change in values of the MAT. This has been shown to be useful for some shape classification and matching purposes [Sundar *et al*., 2003; Sebastian *et al*., 2004; Chang & Kimia 2011].

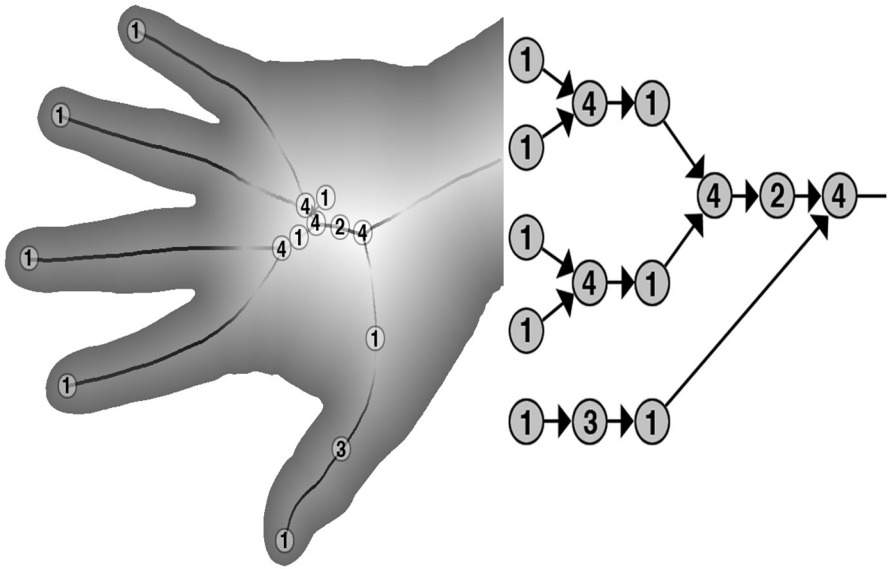

Figure 13. The shock graph representation of the MAT links portions that have monotonically increasing (1), local minimum (2), uniform (3), and local maximum (4) values.

Topology

The skeleton lends itself to several straightforward measurements that provide key descriptive data, which correspond to human visual evaluation of the object shape and may be used for purposes of identification, comparison and correlation. As indicated in Figure 14, the principal topological elements of the skeleton are end points (pixels or voxels with a single neighbor), branches of connected pixels, and nodes (pixels in 2D having more than two neighbors; in 3D, the definitions depend on the connectedness rule in use). There are two kinds of branches possible in a skeleton: internal ones connecting one node to another, and external or terminal branches that have an end point. As shown in the figure, the number of loops in the skeleton can be calculated from Euler's rule (in 3D *Loops = Branches – Ends – Nodes + 2*). For an extended network, as shown below in Figure 30, loops describe the boundaries of the faces of polyhedra in the structure. Counting the number of nodes, ends and branches provides a simple description of the topology of the object. In many cases this provides

a sufficient basis, or at least a few significant variables, that can be used for characterization and identification.

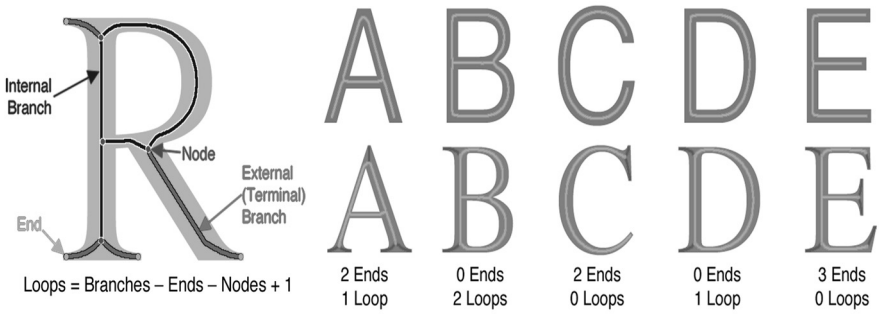

Figure 14. Skeleton of a 2D shape with component parts labeled, and the topological characterization of some letter shapes (red indicates short terminal branches that are removed to eliminate serifs). The letters A through E are distinguishable by the number of loops and ends.

For fonts with serifs, it is necessary to first trim the skeleton by deleting short terminal branches as shown in the figure. This process of trimming to remove short terminal branches is often useful to "clean up" a skeleton if the object has an irregular or rough surface that produces many short external branches [Arcelli & di Baja, 1992]. A threshold for the lengths to trim may be established as a percentage of the total skeleton length or the maximum internal branch length; also, lines that have large angles to continuous segments may be rejected [Shaked & Bruckstein, 1998]. An alternative method to reduce or eliminate spurious branches smooths the object boundary before constructing the medial axis.

On the other hand, short terminal branches have been used to detect dendritic spines as shown in Figure 15. Low density of these has been associated with some neurological conditions [Koh *et al*., 2002; Falcão *et al*., 2002; Wearne *et al*, 2005; Xu *et al*., 2006]. The reduction in spine density characterizes brain damage caused by radiation in space (Figure 15d, e), which affects the ability to learn and remember [Rodriguez *et al*., 2006; Parihar *et al*., 2015].

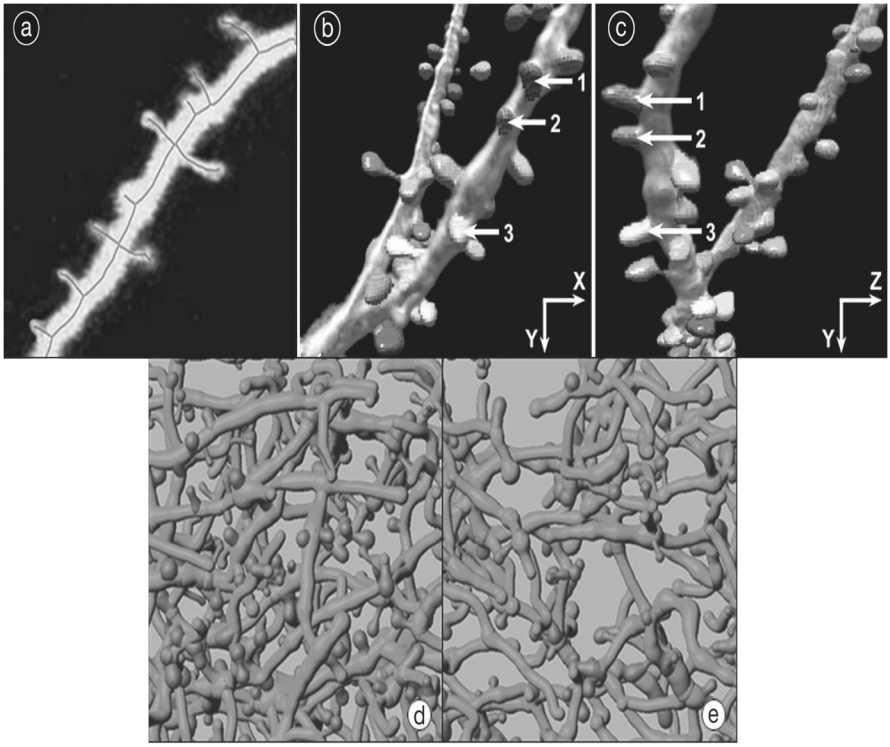

Figure 15. Dendritic spines: a) Skeleton of a dendrite showing the terminal branches marking the spines; b,c) two views of spines reconstructed from the MAT and color coded. The density of spines in mouse prefrontal cortex (d) was reduced after exposure to simulated cosmic ray flux (e).

Skeletons are particularly useful for characterizing the shapes of objects that can flex, bend or otherwise distort their overall appearance. In 3D (Figure 16) they model the shapes of hands as well as the overall form of a person or animal walking, bending, and so forth [Bharatkumar *et al*., 1994]. The topology of the 3D shape is typically well preserved during these alterations, which is not readily evident based on boundary representations such as spherical harmonics or wavelet methods. Measurement of the position, orientation, and curvature of the skeleton branches facilitates analysis of hand motions and horse gaits, and is used to study human walking [Menier *et al*., 2006]. The MAT values typically show only small changes with motion or position [Gal *et al*., 2007] as illustrated in Figure 17, and metric

changes (length, orientation and diameter) may have significant correlations with the pose or motions.

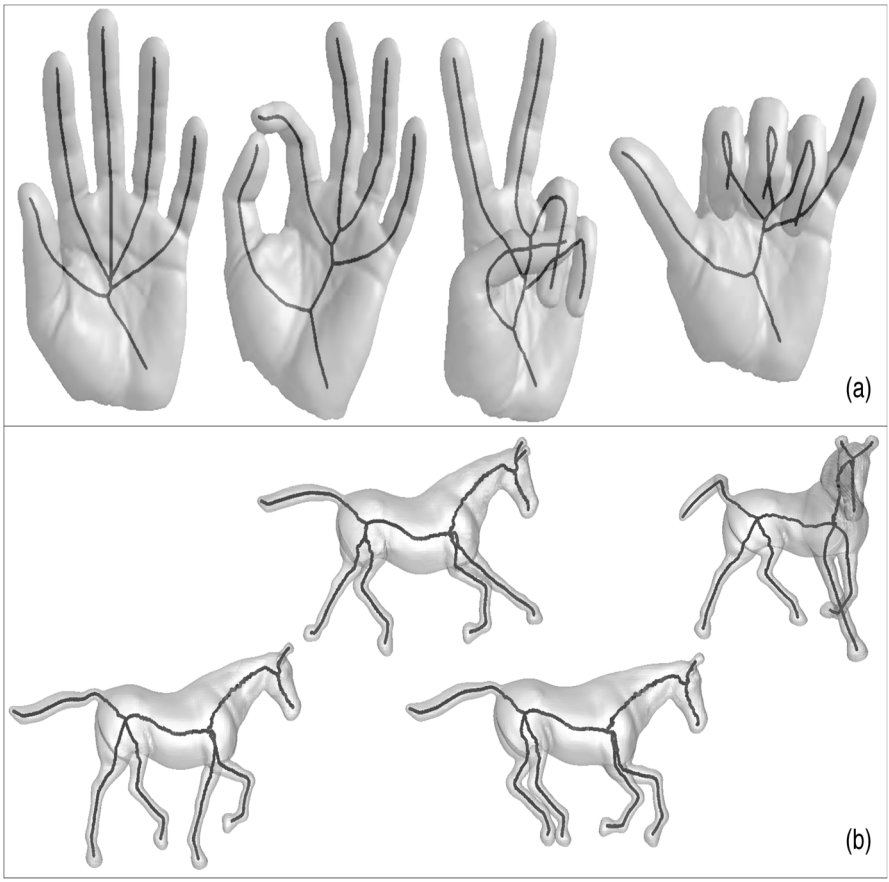

Figure 16. Skeletonization in three-dimensions and its relative invariance with pose: a) hand with 3D skeleton superimposed; b) a horse with the 3D skeleton color coded with distance values.

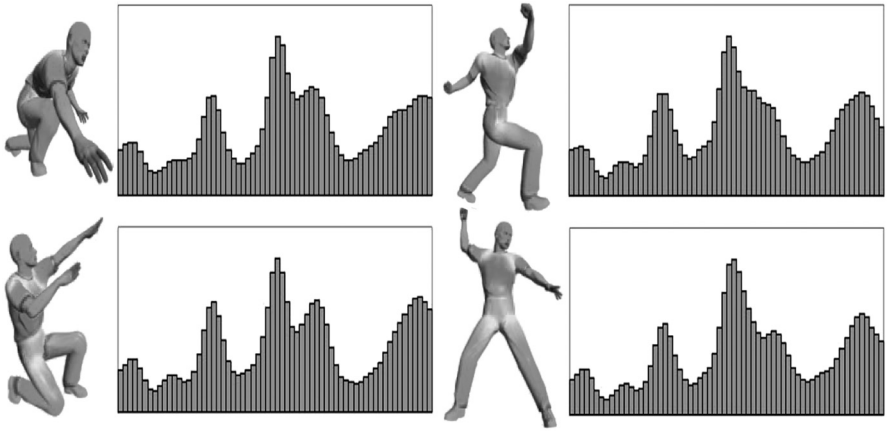

Figure 17. The histogram of MAT values (displayed on the figure surface as distance from the skeleton) varies little with extreme changes in pose.

Changes in the topology are readily identified and tracked, as shown in Figure 18 for a moving amoeba [Xiaong & Iglesias, 2009; Assogba Kokua & Antoine, 2013]. As small "bumps" appear on the boundary, they initially shift the location of the skeleton and if they become larger, result in a new terminal branch forming (pruning may be used to remove "unimportant" branches that arise from minor irregularities). Other measurable properties include the uniformity of branch length, angle, and width, and the spacing and diameter of the local maximum values, which often occur at nodes. All of these properties are readily used for further statistical analysis, for purposes of classification or correlation. Skeleton branching in brain images from tomographic reconstruction has been used to characterize the folding of the brain surface [Naf *et al*., 1995]. The medial axis is used to measure brain structures such as the hippocampus and corpus callosum [Golland *et al*., 1999; Styner *et al*., 2003; Hamarneh *et al*., 2004; Bouix *et al*., 2005; Yushkevic *et al*., 2006] and to compare brains of individuals with autism [Szèkely *et al*., 1992; Gorczowski et al., 2009].

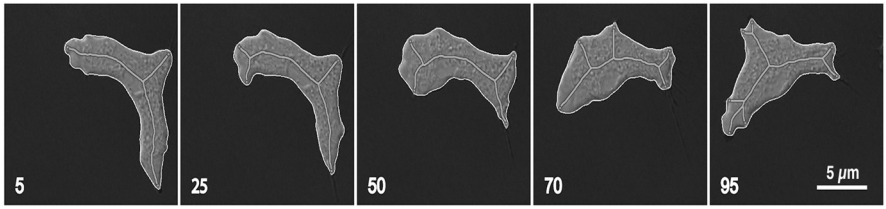

Figure 18. Skeleton of a moving amoeboid cell moving, showing the alteration in the number, position, length and angle of the branches. The elapsed time in seconds is shown in each image.

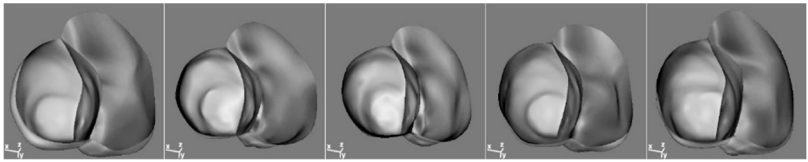

Figure 19. Deformable model of the beating heart based on the medial axis transform, with color coding representing the distance function.

Figure 19 shows the use of the MAT to model the shape and motion of the beating heart [Stetten & Pizer, 1999; Sun *et al*., 2008; Richa *et al*., 2010] with color coding of the surface representing distance from the medial axis. For this purpose, the medial axis is represented by a set of parameters, either in continuous equations or defining piecewise segments, whose values are varied to provide a fit to the heart shape as a function of time. This approach provides a model that can be used to study a shape that varies with time, or to measure and compare a family of similar shapes [Pizer *et al*., 2003]. Deformable models for registration of bones and muscles [Naf *et al*., 1996; Giles *et al*., 2010; Peyrin *et al*., 2010], and the kidney [Shapira *et al*., 2008] have been created using the MAT. This has also been used for registration of CT colonoscopy images [Acar *et al*., 2001] and for alignment and registration to match deformed shapes [Di Ruberto, 2004; Chang & Kimia 2011]. The latter procedures, which match bones and organs to reference shapes, involve manipulations of graphical representations of the 3D MAT. Because of the utility of the medial axis for representing topology, the greatest application of the method has been to branching or network structures such as arteries [Lesage *et al*., 2008]. Visualization of vascular anatomy reconstructed from the MAT has been used for pre-surgical planning to remove tumors [Selle *et al*., 2002].